Cell Medicine, Vol. 7, pp. 95–108, 2015
Printed in the USA.

2155-1790/15 $90.00 + .00
DOI: http://dx.doi.org/10.3727/215517914X680038
www.cognizantcommunication.com

Immature Dental Pulp Stem Cells Showed Renotropic and Pericyte-Like Properties in Acute Renal Failure in Rats

Michele A. Barros,*†[1] João Flávio Panattoni Martins,‡[1] Durvanei Augusto Maria,§ Crisitiane Valverde Wenceslau,* Dener Madeiro De Souza,* Alexandre Kerkis,* Niels Olsen S. Câmara,¶ Julio Cesar C. Balieiro,# and Irina Kerkis*

*Laboratory of Genetics, Butantan Institute, São Paulo, SP, Brazil
†School of Veterinary Medicine and Animal Science, University of São Paulo, São Paulo, SP, Brazil
‡Department of Histology and Embryology, Pontifical Catholic University of Campinas, Campinas, Brazil
§Laboratory of Biochemistry and Biophysics, Butantan Institute, São Paulo, SP, Brazil
¶Department of Immunology, Institute of Biomedical Sciences, University of São Paulo, São Paulo, Brazil
#Department of Basic Science of Faculty of Animal Science and Food Engineering, University of São Paulo, São Paulo, Brazil

Acute renal failure (ARF) is a common renal disease that can lead to high mortality. Recovery from ARF occurs with the replacement of necrotic tubular cells by functional tubular epithelial cells and the normalization of microvascular endothelial cell function in the peritubular capillaries. Conventional therapeutic techniques are often ineffective against ARF. Hence, stem cell therapies, which act through multiple trophic and regenerative mechanisms, are encouraging. We investigated the homing of human immature dental pulp stem cells (IDPSCs) after endovenous (EV) or intraperitoneal (IP) injection, in immunocompetent Wistar rats with ARF induced by intramuscular injection of glycerol, without the use of immunosuppression. The cells, which had been cryopreserved for 6 years, were CD105$^+$, CD73$^+$, CD44$^+$, and partly, STRO-1$^+$ and CD146$^+$, and presented unaltered mesoderm differentiation potential. The presence of these cells in the tubular region of the kidney and in the peritubular capillaries was demonstrated. These cells accelerate tubular epithelial cell regeneration through significant increase of Ki-67-immunoreactive cells in damaged kidney. Flow cytometry analysis confirmed that IDPSCs home to the kidneys (EV 34.10% and IP 33.25%); a lower percentage of cells was found in the liver (EV 19.05% and IP 9.10%), in the muscles (EV 6.30% and IP 1.35%), and in the lungs (EV 2.0% and IP 1.85%). After infusion into rat, these cells express pericyte markers, such as CD146$^+$, STRO-1$^+$, and vascular endothelial growth factor (VEGF$^+$). We found that IDPSCs demonstrate renotropic and pericyte-like properties and contributed to restore renal tubule structure in an experimental rat ARF model.

Key words: Rat; Acute tubular necrosis; Homing; Human immature dental pulp stem cells

INTRODUCTION

Acute renal failure (ARF) affects the function and structure of tubular epithelial cells and provokes microvascular endothelial cell dysfunction in peritubular capillaries. Bone marrow-derived mesenchymal stem cells (BM-MSCs) demonstrate the ability to differentiate into a number of different phenotypes. These cells also demonstrate trophic effects, which are distinct from the direct differentiation of MSCs to repair tissue. Thus, they secrete bioactive factors (paracrine and autocrine) that affect the local cellular milieu, providing repair and regeneration. Such factors suppress the local immune system, inhibit fibrosis (scar formation) and apoptosis, enhance angiogenesis, and stimulate mitosis and differentiation of tissue-intrinsic reparative stem cells (2,3,12,38,39). Kidney tissue-specific stem cells are a practical choice for renewing damaged tissues in ARF. However, the methods for their isolation and expansion are still under investigation (15,17,22). The complexity of the anatomic organization and function of the kidneys, which involve more than 14 different cell types, warrants the importance of studying cell-based therapies using different cell types. Among these cell types are progenitor cells from the kidneys, endothelial cells, BM-MSCs, amniotic fluid stem cells, and predifferentiated pluripotent stem cells, either embryonic or induced (18,19,28,30,31). These stem cell types are similar, but not equivalent, to BM-MSCs. Therefore, it is not clear if they will act as trophic mediators providing additional benefits in stem cell therapy.

Dental pulp of deciduous teeth presents an almost unlimited source of young stem cells, providing easy access and

Received August 16, 2013; final acceptance February 20, 2014. Online prepub date: March 24, 2014.
[1]These authors provided equal contribution to this work.
Address correspondence to Dr. Irina Kerkis, Laboratório de Genética, Instituto Butantan, Av. Vital Brasil 1500, SP, CEP 05503-900.
Tel: +5511 26279705; E-mail: irina.kerkis@butantan.gov.br

minimal ethical concerns. Human immature dental pulp stem cells (IDPSCs) were isolated from the dental pulp of deciduous teeth (25). Ex vivo expansion of IDPSCs leads to the isolation of a multicellular population, standardized with respect to expression of several mesenchymal markers such as cluster of differentiation 105 (CD105, SH2 clone), which is important for angiogenesis (11), CD73 (SH3), CD29 (integrin b-1), vimentin, and others. IDPSCs are multipotent and, after reprogramming into induced pluripotent stem cells, produce teratomas in mice. These can differentiate into multiple tissues, among which immature nephron-like structures were also observed (1,25). In contrast to BM-MSCs these IDPSCs are a highly enriched population of neural crest cells, which express such markers as nestin, sex-determining region Y box 2 (SOX2), and the low-affinity tumor necrosis factor (TNF) receptor, p75 (26).

Several groups have demonstrated that the injection of stem cells could contribute to recovery from ARF, when experimentally induced by intramuscular administration of glycerol (7,20,21,27). The aim of the present study was to answer several questions: (a) whether cryopreserved human IDPSCs, maintained for 6 years and injected endovenously (EV) or intraperitoneally (IP), may survive, proliferate, migrate, and home to the tubular epithelial tissue and peritubular capillaries in immunocompetent Wistar rats with glycerol-induced ARF; (b) whether IDPSCs can act as trophic mediators and express in vivo (after transplantation) pericyte markers such as CD146, STRO-1, and vascular endothelial growth factor (VEGF), important for their target homing to the kidneys; (c) whether IDPSCs will accelerate tubular epithelial cell regeneration; and (d) whether IDPSCs graft in the kidneys, or if they "escape" from the principal renal route of migration and also graft in the liver, muscle, and lungs.

MATERIALS AND METHODS

Cell Culture

The IDPSCs used in this study were obtained previously, from the dental pulp of deciduous teeth of a 6-year-old individual (male), fully characterized, and stored in liquid nitrogen for 6 years (25). After thawing the IDPSCs (37°C, 3 min), 10^6 cells at passages 3–4 were seeded into flasks (150 cm^2; Corning, Corning, NY USA) in Dulbecco's modified Eagle's medium (DMEM)/Ham's F12 (1:1; Invitrogen, Carlsbad, CA, USA), supplemented with 15% fetal bovine serum (FBS; HyClone, Logan, UT, USA), 2 mM glutamine (Gibco, Gaithersburg, MD, USA), 50 mg/ml gentamicin sulfate (Schering-Plough, Whitehouse Station, NJ, USA), and 1% nonessential amino acid (Gibco) and were expanded for two to three more passages. The medium was refreshed every 2 days and grown until reaching semiconfluence (80–90%). All cell cultures were maintained at 37°C in a 5% CO_2 high-humidity atmosphere.

Growth Curves

Growth kinetics analysis of the IDPSCs was performed after thawing. These cells, starting from passage 4, were grown in DMEM/Ham's F12, supplemented with 15% FBS, 2 mM glutamine, 50 mg/ml gentamicin sulfate, and 1% nonessential amino acid to reach semiconfluence. Cells were then trypsinized (Invitrogen), stained with trypan blue solution 0.4% (Sigma-Aldrich, São Paulo, SP, Brazil), and counted using a Neubauer chamber (Thomas Scientific, Swedesboro, NJ, USA). Cells were seeded in a new flask at 1×10^5 cells/cm^2. Next, IDPSCs were harvested every third day, trypsinized, and counted for nine passages. Three separate growth experiments were performed. Growth curves of IDPSCs before thawing, used for comparison, were adopted from previous publications (25).

Immunophenotyping

Immunofluorescence analyses were performed, before IDPSC infusion into rat ARF models. These cells (passage 5–6), were grown on coverslips (Biosystems, São José dos Pinhais, Parana, Brazil) in basal culture medium for 48 h, washed twice in Tris-buffered saline (TBS) containing 20 mM Tris-HCl (Vetec, Duque de Caxias, Brazil), pH 7.4; 0.15 M NaCl (Dinâmica Reagent, São Paulo, Brazil), and 0.05% Tween-20 (Sigma-Aldrich) and fixed for 24 h in 4% formaldehyde (Gardem Química, Guarulhos, SP, Brazil), following permeabilization with 0.1% Triton X-100 (Sigma-Aldrich). After blocking with 5% bovine serum albumin (BSA; Sigma-Aldrich), the cells were incubated for 1 h at room temperature with primary antibodies diluted in BSA. The primary antibodies used for the immunophenotypic profile were anti-mouse vimentin and anti-human nestin (both 1:200; from Santa Cruz Biotechnology, Santa Cruz, CA, USA). After washing the cells three times in TBS (0.01 M, pH 7.4; Gibco), fluorescein isothiocyanate (FITC)-conjugated antibodies (1:500) were added, and the cells were incubated for 40 min at room temperature. The secondary antibodies used were anti-gouti IgG (Santa Cruz Biotechnology) and anti-mouse IgG (Amersham Biosciences, Piscataway, NJ, USA). Microscope slides were mounted in Vectashield mounting medium, with or without 4′,6-diamidino-2-phenylindole (DAPI; Vector Laboratories, Burlingame, CA, USA).

Flow Cytometric Analysis

For flow cytometric analysis of IDPSCs after cryopreservation, the following antibodies against cell surface molecules and their respective isotype controls were used: monoclonal anti-human CD45 (1:50; Sigma-Aldrich), anti-human CD90, anti-human CD146 (both 1:50; from BD-PharMingen, San Diego, CA, USA), anti-human CD105 (SH2), anti-human CD73 (SH4; both 1:100; from Case Western Reserve University, Cleveland, OH, USA), anti-human STRO-1 (1:50; R&D Systems, Minneapolis,

MN, USA), and VEGF (1:50; Sigma-Aldrich). About 1×10^6 cells were incubated on ice with primary antibody for 2 h, washed in phosphate-buffered saline (PBS; (0.01 M, pH 7.4; Gibco) + 2% FBS and 1 M sodium azide (Sigma-Aldrich), followed by the addition of secondary FITC-, phycoerythrin-, and rhodamine-conjugated antibodies (1:500; all from Thermo Fisher Scientific Inc. Waltham, MA, USA), respectively. Cells were incubated with a secondary antibody overnight. Next, only the incubated STRO-1 cells were resuspended in 1 ml of Tween-20 solution (0.2% in PBS; Sigma-Aldrich) at room temperature, and the mixture was incubated for 15 min in a 37°C water bath. Flow cytometry analysis was performed using a fluorescence-activated cell sorter (FACSCalibur; Becton Dickinson, San Jose, CA, USA) with the CELL Quest program (Becton Dickinson).

In Vitro Differentiation

To promote osteogenic differentiation, the IDPSCs were cultured in an osteogenic medium composed of DMEM-LG (Invitrogen), 2% FBS (Invitrogen), 50 mM ascorbate-2-phosphate (Invitrogen), and 0.1 mM dexamethasone (Sigma-Aldrich), and the culture medium was changed every 3 days. After 10 days, the osteogenic medium was supplemented with 10 mM β-glycerol phosphate (Sigma-Aldrich). At day 21, the cells were washed twice in PBS, fixed for 24 h in 4% formaldehyde (Gardem Química), and stained with the von Kossa reagent (Invitrogen).

Adipogenic differentiation was performed according to the protocol for human adipose tissue-derived cells (MSCs) (40). Cells were cultivated, and adipogenic differentiation was induced by the addition of DMEM-HG (Invitrogen) supplemented with 2% FBS (Invitrogen), 1 mM dexamethasone, 100 mM indomethacin, 0.5 mM 1-methyl-3-isobutyxanthine, 10 mg/ml insulin, and 10,000 µg/ml antibiotics (all Sigma-Aldrich). The medium was changed every 3 days. At day 10, differentiated cells were washed twice in PBS and fixed as described above. Oil red O (Sigma-Aldrich) staining was used to detect intracellular lipid accumulation.

Chondrogenic differentiation was carried out using a pellet culture technique (23). Pellets of IDPSCs were resuspended in a culture medium containing DMEM-HG supplemented with 6.25 mg/ml insulin, 6.2 mg/ml transferrin, 6.25 mg/ml selenous acid, 5.33 mg/ml linoleic acid (ITS Premix; BD Biosciences, San Jose, CA, USA), 0.1 mM dexamethasone, 1 mM sodium pyruvate (Sigma-Aldrich), and 50 mg/ml ascorbate-2-phosphate. The cells were maintained at 37°C in a humidified atmosphere with 5% CO_2 for 21 days, and the chondrogenic culture medium was changed every day. After 21 days, cell aggregates were embedded in paraffin (Media-Paraplast Plus®; Oxford Labware, St. Louis, MO, USA). Sections (4–5 µm) were cut using a Leica microtome (Wetzlar, Germany) and were stained with toluidine blue (Sigma-Aldrich), following routine protocols.

Acute Renal Injury in Wistar Rats and Treatment

All studies were approved by the ethics committee of the School of Veterinary Medicine and Animal Science, University of São Paulo. The experiments were performed in accordance with the guidelines established by the Butantan Institute for Animal Experimentation. ARF in Wistar outbred rats ($n=16$; Central Animal Facility of the Butantan Institute, São Paulo, SP, Brazil) was induced by rhabdomyolysis as described elsewhere (41). Eight-week-old male rats weighing 200–300 g were housed in temperature-controlled conditions under a light/dark photocycle with food and water supplied ad libitum. The animals were divided into two major groups: (A) control ($n=4$); (B) experimental injury induction by glycerol injection ($n=12$). Group B was subdivided into (B1) control saline injection ($n=4$); (B2) intraperitoneal (IP) IDPSC transplantation ($n=4$); and (B3) endovenous in caudal vein (EV) IDPSC transplantation ($n=4$). First, the experimental group was dehydrated for 12 h before glycerol injection, and the animals were anesthetized with 70 mg/kg ketamine (Dopolen®) and 7 mg/kg xylazine (Anasedan®) (both from Vetbrands, Jacareí, SP, Brazil). Then, acute renal injury was induced by intramuscular injection of 50% glycerol (6 ml/kg; Sigma-Aldrich) into the rats' lower hindlimbs. Twenty-four hours later, animals from subgroup B1 were submitted to EV saline injection and the other subgroups, B2 and B3, to IP and EV IDPSC transplantation (7×10^5 in 0.5 ml of saline vehicle solution), respectively. All animals were sacrificed 2 days after the IDPSC transplantation, using a high concentration of 150 mg/kg ketamine and 15 mg/kg xylazine (Fig. 1). Kidney tissue was fixed in 10% formaldehyde (Garde Quimíca) or frozen in OCT (Tissue-Tek; Sakura FineTek, Torrance, CA, USA).

Immunohistochemistry

To confirm the origins of the IDPSCs in the kidney sections of the injected mice, the slides were stained with anti-human-IDPSC (immature dental pulp stem cells) (Butantan-Institute, SP, Brazil) and anti-human nucleus (hNu) (Millipore Corporation, Billerica, MA, USA) antibodies. The method for polyclonal anti-IDPSC antibody production with specificity for human IDPSCs was previously reported (25), as well as used in other several publications (16). First, the paraffin slides were deparaffinized using a routine technique. Then, the slides were incubated with ammonia hydroxide (Sigma-Aldrich) for 10 min and washed four times in distilled water for 5 min each. Antigen retrieval of the slides was performed using a pH 6.0 buffer of sodium citrate (Sigma-Aldrich), in a water bath set at 95°C for 35 min. The slides were

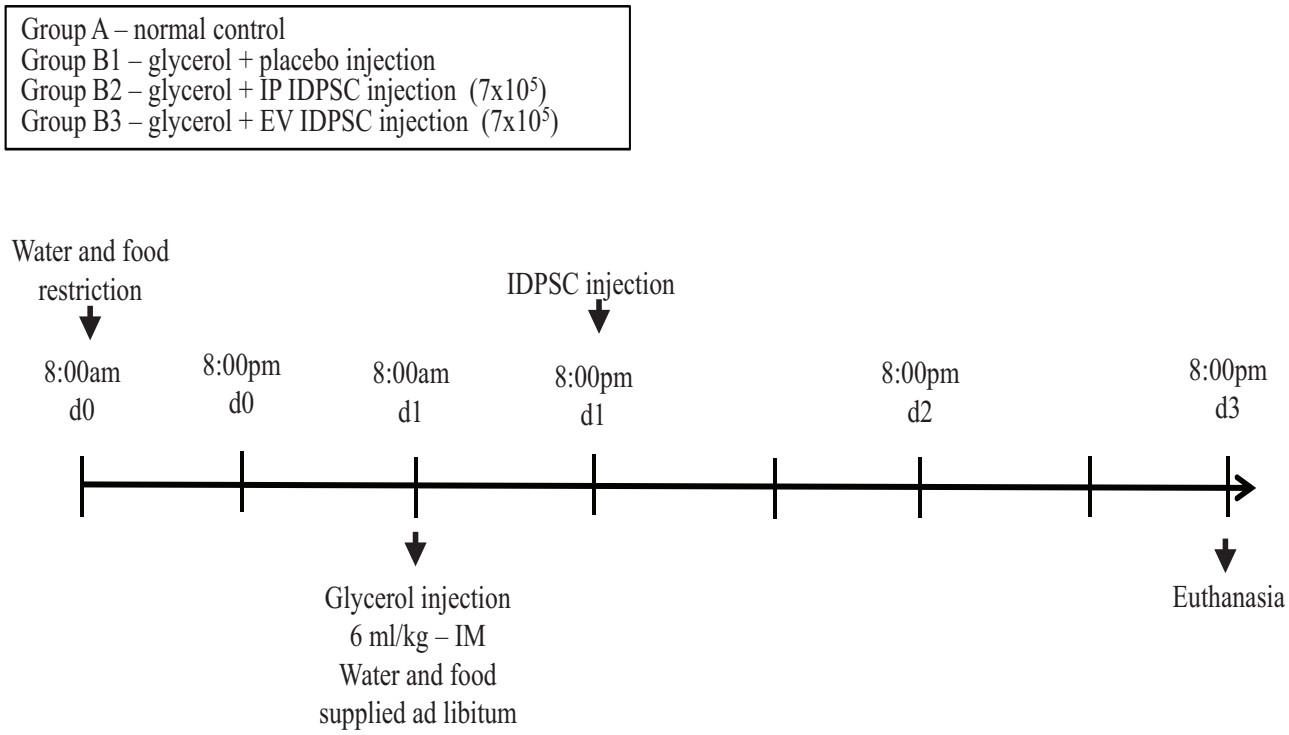

Figure 1. Schematic representation of the protocol of glycerol-induced ARF and treatment with IDPSCs. Day 0 (d0) – 8:00 pm: water and food restriction. Day 1 (d1) – 8:00 am: glycerol injection. Day 1 (d1) – 8:00 pm: immature dental pulp stem cell (IDPSC) (7×10^5) or placebo injection. Day 3 (d3) – 8:00 pm: animal sacrifice. ARF, acute renal failure; IP, intraperitoneal; EV, endovascular.

blocked with hydrogen peroxide (Sigma-Aldrich) for 15 min and incubated overnight at 4°C with primary antibodies diluted in BSA (Sigma-Aldrich). The primary antibodies used for the immunophenotypic profile were anti-IDPSC (1:100; Butantan Institute, SP Brazil) and anti-human nucleus (1:20; hNu; Millipore Corporation). Then, the slides were rinsed three times with PBS for 5 min each, and anti-mouse secondary antibody (1:500) and ready-to-use Envision kit (DakoCytomation, Milan, Italy) were added for 40 min at room temperature. The same procedure was used for Ki-67 (1:50; Sigma-Aldrich) immunostaining. Afterward, the slides were washed three times in PBS for 5 min each. Finally, diaminobenzidine (DAB; DakoCytomation) was applied to produce brown anti-IDPSC and anti-hNu staining. The immunostained sections were counterstained with hematoxylin (Sigma-Aldrich), to be observed under a light microscope (Axio Observer; Zeiss, Jena, Germany).

CFSE-Labeled IDPSCs

To evaluate the engraftment of the IDPSCs after IP and EV injection into mice, the IDPSCs were labeled using a Vybrant CFDA SE Cell Tracer Kit (CFSE; 5-(and-6)-carboxyfluorescein diacetate, succinimidyl ester; Invitrogen). Kidney tissues were embedded into OCT. Frozen sections (5 μm) were obtained using a cryomicrotome (Cryostat CM1100; Leica) and placed on poly-L-lysine-coated slides (Sigma-Aldrich), which were incubated in cold methanol (Sigma-Aldrich) for 15 min to decrease tissue autofluorescence. Afterward, they were washed three times in rinse buffer (TBS and 0.05% Tween-20). Finally, slides were mounted in an antifade solution (Vectashield mounting medium) and analyzed by fluorescent microscopy (Axio Imager A1; Carl Zeiss, São Paulo, Brazil) or confocal microscopy (LSM 510 META; Carl Zeiss). An argon ion laser set at 488 nm for FITC (Chemicon, Temecula, CA, USA) and at 536 nm for cyanine 3 (Cy3; Chemicon) excitation was used. The emitted light was filtered with a 505-nm (FITC) and 617-nm (Cy3) long pass filter in a laser scanning microscope.

Flow Cytometric Analysis of Tissues After Transplantation

To estimate the incorporation of IDPSCs and any eventual loss of the cells after transplantation by both routes of administration into kidney and other tissues, such as muscle (injury site), liver, and lung, the expression of stem cell markers (CD45, CD90, CD146, IDPSC, STRO-1, and VEGF) was analyzed through cytometry analysis. In order to produce single cells, disaggregation with 0.1% collagenase (Gibco) was performed on the solid tissue

for 10 min. Following suspension, this was centrifuged at $106 \times g$ for 10 min. Cell pellets that were formed were resuspended in 3 ml of ligation buffer (Ca, glycine, Mg, pH control factor without phenol; Sigma-Aldrich). Then the cell pellets were counted using trypan blue and a hemocytometer (Laboroptick, Lancing, UK). About 1×10^6 cells were incubated for 2 h on ice with primary monoclonal antibodies: anti-human IDPSC (1:200), anti-human CD45 (1:50; Sigma-Aldrich), anti-human CD90, anti-human CD146 (both 1:50; from BD-PharMingen), anti-human CD105 (SH2), anti-human 73 (SH4; both 1:200; from Case Western Reserve University), anti-human STRO-1 (1:50; R&D Systems), and anti-VEGF (1:50; Sigma-Aldrich). Afterward, the cell pellets were washed in PBS and 1 µM sodium azide (Sigma-Aldrich). Then anti-mouse secondary FITC, phycoerythrin, and rhodamine (1:500; all from Thermo Fisher Scientific Inc.) were added to the conjugated antibody for 2 h at room temperature. Only the incubated STRO-1 cells were resuspended in 1 ml of Tween-20 (Sigma-Aldrich) solution (0.2% in PBS) at room temperature, and the mixture was incubated for 15 min in a 37°C water bath. Flow cytometry analysis was performed, using a fluorescence-activated cell sorter (FACS; Becton Dickinson) with the CELL Quest program. The expression of the markers was determined by comparison with an isotope control, following statistical analysis (below).

In order to quantitatively analyze Ki-67-immunoreactive cell numbers, 15 sections per each animal were selected. Images of all Ki-67-immunoreactive cells were taken through a light microscope (Olympus, Tokyo, Japan) equipped with a digital camera (DP71, Olympus) connected to a PC monitor. The number of Ki-67-positive cells in the kidney was counted by Optimas 6.5 software (Cyber Metrics, Scottsdale, AZ, USA). Cell counts were obtained by averaging the counts from the sections taken from each animal: a ratio of the count was calibrated as percent.

Histology

Renal tissues were fixed in 10% formaldehyde (Gardem Química), dehydrated, and embedded in paraffin. For general histology, sections were sliced (5 µm) and stained with hematoxylin and eosin (H&E; Merck, Darmstadt, Germany). In addition, some kidneys were frozen in liquid nitrogen using OCT (Tissue-Tek; Sakura FineTek) and stored at −220°C.

When required, kidneys were cryosectioned at 5 µm and then used for confocal microscopy investigation of IDPSCs marked with Vibrant Tracer (V12883; Invitrogen).

Statistical Analyses

To evaluate the percentage of IDPSCs present in the kidneys, muscles (injury site), liver, and lungs from IP and EV injection in mice, a completely randomized design (CRD), in a factorial 4×4 arrangement, was adopted, according to the model specified below:

$$Y_{ijk} = \mu + R_i + O_j + RO_{ij} + e_{ijk}$$

where Y_{ijk} = the observed value for the percentage of IDPSCs in replication k, in route of administration j and in organ i; μ = the constant for all observations (mean); R_i = effect of the ith organ, being $i = 1$ (kidneys), 2 (muscles-injury site), 3 (liver), and 4 (lungs); O_j = effect of the jth route of administration, being j = A (control), B1 (glycerol control saline injection), B2 (IP IDPSC transplantation), and B3 (EV in caudal vein IDPSC transplantation); RO_{ij} = effect of the double interaction between route of administration i with organ j; e_{ijk} = experimental error associated with variable percentage of IDPSCs in replication k, in route of administration j and in organ i, assuming normally, identically, and independently distributed (NIID; 0, σ^2_e).

For this statistical model, since significant effects were observed for the double interaction, the developments were conducted using Tukey's post hoc test within each route of administration and within each organ. All tests were performed with the aid of the Statistical Analysis System© (SAS 2005; SAS Institute, Cary, NC, USA), using the PROC MIXED procedure.

RESULTS

IDPSC Characterization After Cryopreservation

The human IDPSCs remained frozen in liquid nitrogen for about 6 years; therefore, before their injection into the experimental animals, the original characteristics of the preserved cells were verified. After thawing, these cells showed typical MSC morphology and a good growth rate (Fig. 2A, B). Flow cytometry demonstrated a high number of IDPSCs positive for (MSC) surface antigens, (Fig. 2C–F) such as CD105 (SH2; 96.4%) and CD73 (SH4; 98.6%), and were also positive for STRO-1 (28%) and CD146 (36%), markers of pericytes and BM-MSCs (13). Additionally, IDPSCs were negative for CD45 and CD90 (Fig. 2G, H). A very small amount of IPDSCs (3.65%) were positive for VEGF (Fig. 2I). Differentiation capacity of IDPSCs into bone, cartilage, and adipose cells was also verified and was as shown previously (26).

Morphological Analysis

Histological analyses of the kidney tissues of animals from each group are shown in Figures 3 and 4. Kidney tissues in those animals with ARF induced by glycerol revealed a marked dilatation of the renal cortical tubules, proximal tubular epithelium necrosis (no nuclei, intense eosinophilic homogeneous cytoplasm, but preserved shape), and accumulation of cellular debris in the tubular lumen (Fig. 3A1–C1).

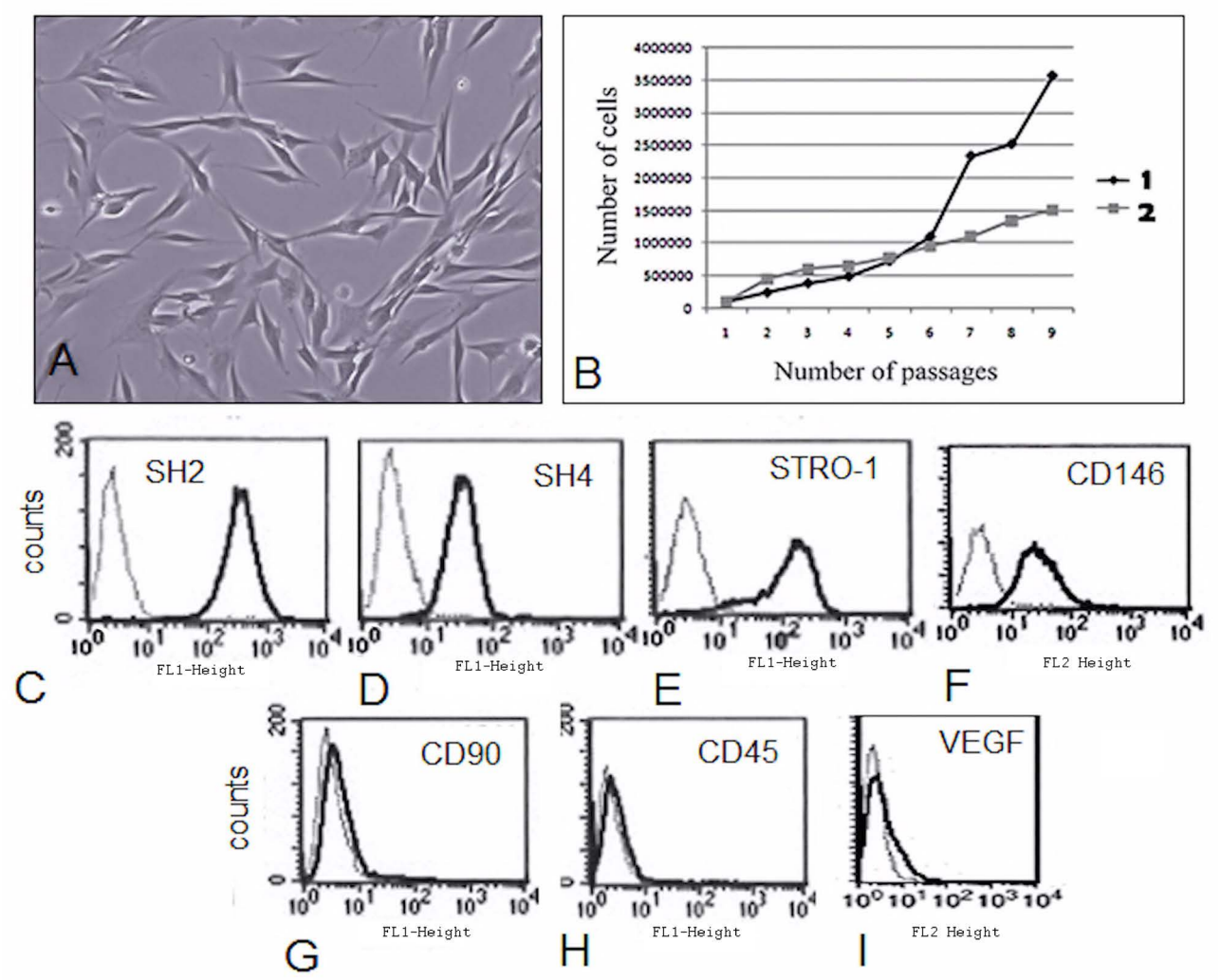

Figure 2. Characterization of IDPSCs after 6 years of cryopreservation. (A) Morphology. (B) Proliferative rate of IDPSCs: (1) 6 years earlier; (2) currently, after thawing. (C–I) Immunophenotyping of IDPSCs after thawing. (C–F) Positive reactions of IDPSCs with antibodies such as cluster of differentiation 105 (CD105; SH2 clone), CD73 (SH4 clone), STRO-1, and CD146, respectively. (G, H) Lack of reaction of antibodies CD90 and CD45 with IDPSCs (negative control). (I) A small number of IDPSCs demonstrated immunopositivity for vascular endothelial growth factor (VEGF).

In the IP and EV IDPSC injection groups (B2 and B3, respectively), the presence of vascular congestion, characterized by active hyperemia resulting in arterial dilation, was observed. Increased blood flow in the capillaries was also detected (Figs. 3A2–C2, A3–C3 and 4A2–C2, A3–C3). These characteristics are particularly distinct in blood vessels present in the medulla (Fig. 4A2–C2, A3–C3). However, it seems that they are even more pronounced in the B3 group, when compared with the B2 and control groups (Fig. 3B3).

Detection of Incorporation of IDPSCs Into Tubular and Perivascular Regions of Kidney

Two methods were used to analyze the migration and incorporation of IDPSCs into the tubular and perivascular regions of the kidneys in ARF. First, the cells (7×10^5) were stained with fluorescent dye (CFSE Cell Tracer Kit—red). This allows clear discrimination of stained cells from possible background, within the analyzed tissue, during microscopic visualization. After IP injection, the IDPSCs (group B2) had partially been incorporated into the tubular epithelium (Fig. 5A–D). A similar, but not identical, pattern of localization of IDPSCs within the kidney was detected after EV injection in group B3 (Fig. 5E–H). The cells were detected in the glomerulus (Fig. 5E–E2) and in the endothelial layer of small blood vessels surrounding the tubular integrity of the injured kidney (Fig. 5F) and in the intertubular space (Fig. 5G).

Next, immunohistochemical detection of IDPSC incorporation was performed using two anti-human

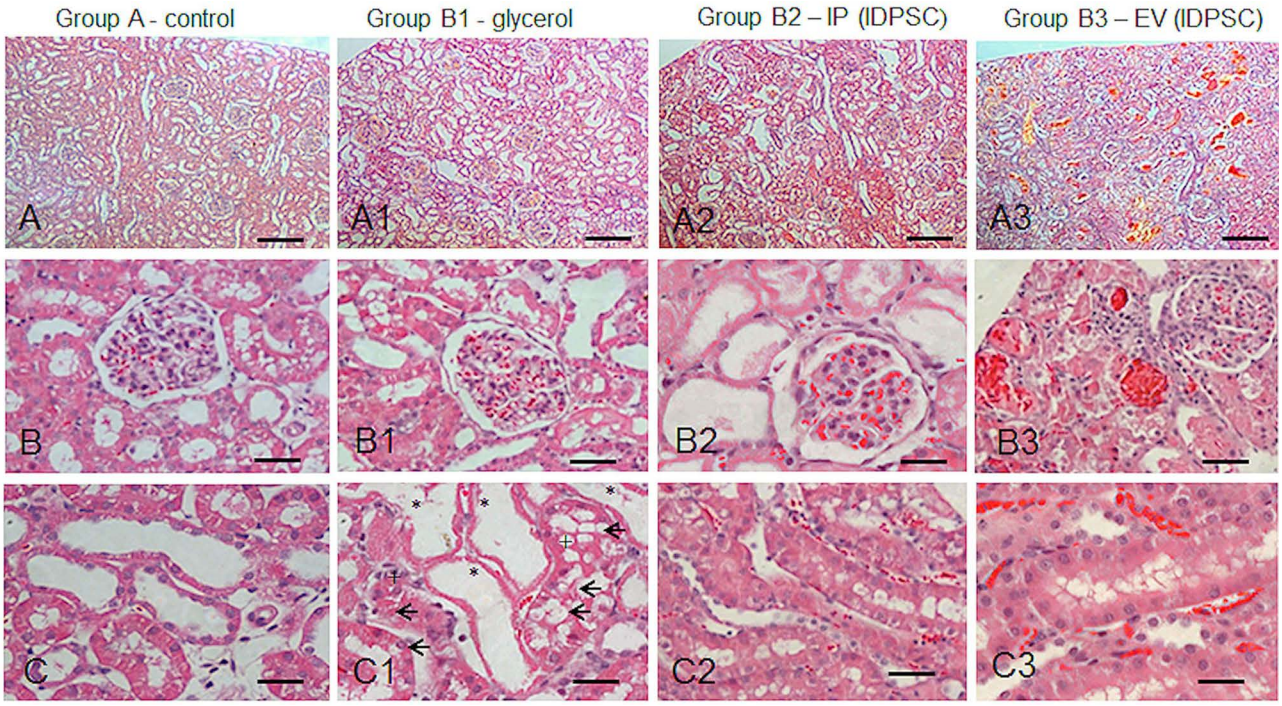

Figure 3. Morphological aspects of renal cortex: normal (A–C); ARF (A1–C1) and after IDPSCs IP (A2–C2) and EV (A3–C3) transplantation. (A1–C1) ARF characteristics, such as renal cortical tubules dilatation with flattened or peeling epithelium (*), cellular debris in tubular lumen (+), and degenerative tubular cells (arrows). (A2–C2) and (A3–C3) Modest morphological amelioration can be observed in comparison with (A1–C1). Note the vascular congestion and increased blood flow in the capillaries, which was more pronounced in the EV route (A3–C3). Light microscopy, hematoxylin and eosin (H&E) staining. Scale bars: A–A3: 100 μm; B–C3: 50 μm.

cell antibodies: anti-nucleus (hNu) and anti-IDPSC. Accordingly, after IP injection, multiple human nuclei were detected in the intertubular space (Fig. 5I, J, and L) and in tubules close to the glomerulus (Fig. 5K). A similar pattern of localization of IDPSCs within the kidney in the tubular epithelium was detected after EV injection (Fig. 5M, N). Respective controls are presented in Figure 5O and P.

Since injury can also occur in the muscles of a region of glycerol application, we verified possible IDPSC migration to this site. Several positively immunostained human nuclei were found sandwiched between the basement membrane and the sarcolemma of individual muscle fibers (Fig. 5Q), adjacent to satellite cells.

Effects of IDPSC Transplantation on Kidney Cell Proliferation

In the B2 and B3 groups, Ki-67-immunoreactive cells were detected (Fig. 6A, B). The number of Ki-67-immunoreactive cells was significantly increased by 15% (IP) and 28% (EV) after IDPSC injection compared with A and B1 groups (Fig. 6C, D). In these groups, the number of Ki-67-immunoreactive cells was 5% and 2%, respectively.

Flow Cytometry Analysis

In addition to the kidneys, other tissues, including muscle (injury site), liver, and lung, were analyzed with respect to IDPSC incorporation, in order to evaluate any eventual loss of cells after transplantation, by both routes of administration. Several markers, which were found to be unexpressed (CD45, CD90) or expressed (CD146, STRO-1) in undifferentiated IDPSCs, have been tested in recipient rat tissues after cell transplantation (Figs. 7 and 8). Expression of anti-IDPSC antibody, which was used for immunohistochemical detection of these cells in renal tissues (Fig. 7), was also analyzed using flow cytometry in all tissues. Additionally, the expression of VEGF, which is a signal protein that stimulates vasculogenesis and angiogenesis, was evaluated.

No expression of any analyzed markers was observed in either control group, which did not receive the cells (Figs. 7 and 8). The expression of anti-IDPSC antibody revealed an abundant incorporation of these cells into the kidneys (Fig. 7). Expression of CD146 (marker for pericytes) and STRO-1 (marker for stromal cell precursors in human bone marrow) (34) demonstrated that, just after injection, a population of IDPSCs consists of undifferentiated cells. VEGF expression suggests that IDPSCs may

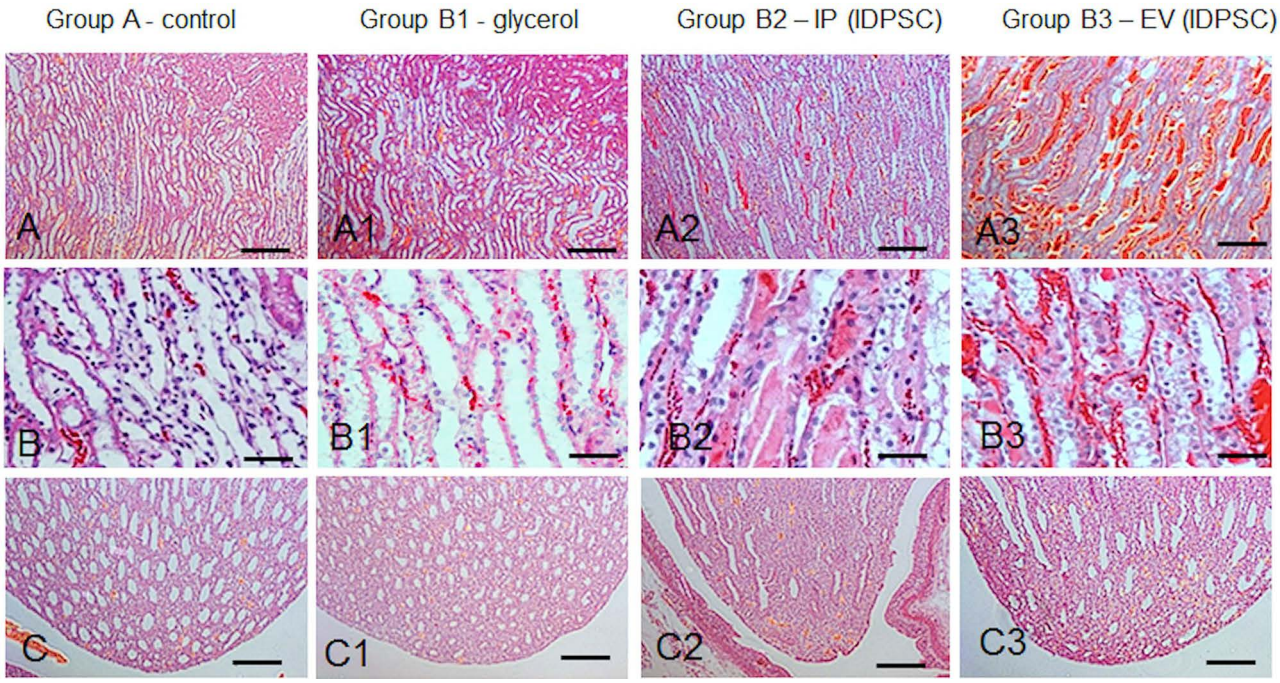

Figure 4. Morphological aspects of renal medullary regions (A–B3) outer zone, and (C–C) renal papillae): control (A–C) normal animals; ARF (A1–C1) and after IDPSC IP (A2–C2) and EV (A3–C3) transplantation. (A1–B1) Discrete ARF characteristics, such as tubular dilatation with flattened or peeling epithelium. (A2–B2) and (A3–B3) Modest morphological amelioration can be observed in comparison with (A1–B1). Note the vascular congestion and increased blood flow in capillaries (A2–B3), which was more pronounced in the EV route (A3–B3). (C1–C3) No significant alterations were observed in comparison with (C). Light microscopy, H&E staining. Scale bars: 100 μm (A–A3, C–C3); 50 μm (B–B3).

stimulate angiogenic activity in kidney tissues. No significant difference in expression of any of these markers, by the two routes of administration (IP and EV), was noted (Table 1). As expected, CD45 (marker for hematopoietic cells) and CD90 (marker for primitive hematopoietic stem cells), used as controls, were not found to be expressed in the kidney tissues (Fig. 7).

IDPSC incorporation was lower in muscle tissue than in the kidneys, and the EV route seems to be more efficient in delivering cells when compared to the IP route (Fig. 7 and Table 1). Antibodies for CD146 and STRO-1 were found to be expressed in the liver (Fig. 8). However, anti-VEGF and anti-IDPSC-positive cells showed significantly higher percentages ($p<0.01$) in the kidneys than in the liver (Table 1). In lung tissue, anti-IDPSC antibody or other positive cell markers have been presented marginally (Fig. 8).

Statistical Analysis

Considering the proposed model, analysis of variance (ANOVA) for the different antibodies revealed a significant effect ($p<0.01$) for the source of variation, which is related to the interaction between the application route (V) and the tissues of application (O). The extent of the interactions for the different antibodies showed a similar pattern of results. Nonsignificant ($p>0.05$) effects were observed for muscle and lungs, while significant effects were shown for the liver and kidneys ($p<0.01$) (Table 1).

DISCUSSION

ARF shows vascular, inflammatory, and tubular injuries. Owing to the complexity of ARF, current techniques, such as dialysis and pharmacological or hormonal therapies, have had no significant impact on patient survival, since these approaches often affect only one factor of multiple organ damage (21,26,36). Stem cell therapies, which act through multiple mechanisms such as anti-inflammatory, antiapoptotic, immunomodulation, and others (4), appear to be an advantageous therapeutic approach for ARF (18, 19,21,24,26,28,30,32,33,37). The finely drawn choice of stem cells for each type of injury and disease is a challenge in modern cell therapy. The viability of cells, after a long period of cryopreservation, is essential for successful stem cell therapy. Our data showed that IDPSCs, even after a long period of cryopreservation, remained with their characteristics preserved. This makes them an attractive type of stem cell for future therapies.

Next, an expression of specific markers is important for stem cell migration and target homing, directed at damaged organs. Exogenous $CD44^{+}$ BM-MSCs showed

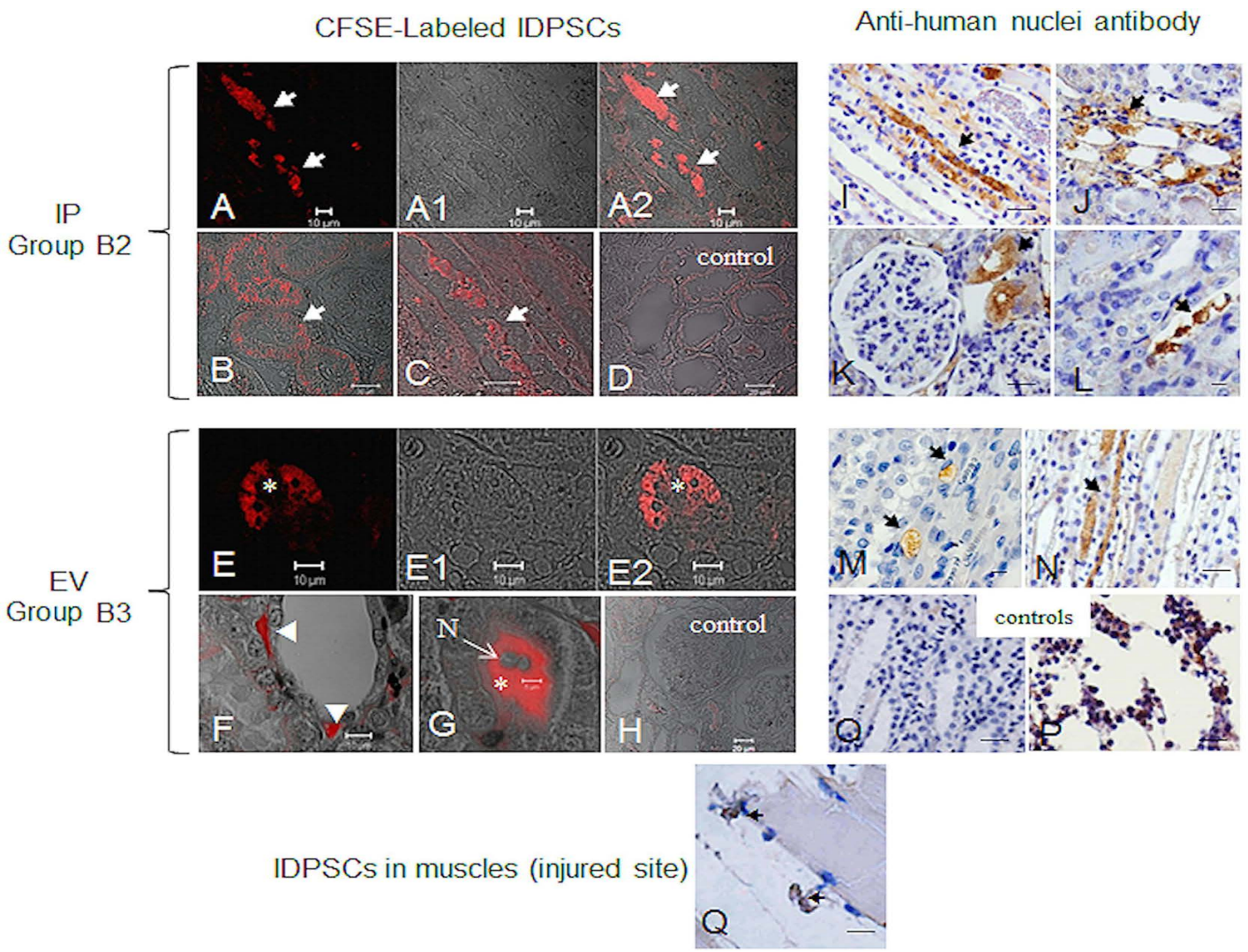

Figure 5. IDPSC homing in ARF rat kidneys demonstrated by two different assays: (A–H) Fluorescently labeled IDPSCs; (I–P) using anti-human nuclei antibody. (A–D) and (I–L) IDPSC homing was demonstrated in the B2 group—IP transplantation. (A–A2, B, and C) Localization of IDPSCs in tubular epithelium is observed (white arrows). Similar localization of IDPSCs was observed in (I–L) (black arrows). (E–E2) IDPSCs are localized in the glomerulus (white asterisk). (F) IDPSCs were found in small blood vessels (white arrowheads). (G) IDPSCs presenting typical fibroblast-like morphology were found in the intertubular space (white asterisk). (D and H) The negative control rats were injected with saline solution. (M and N) The presence of IDPSCs in tubular epithelium is demonstrated (black arrows). (O) Negative control (primary antibody was omitted). (P) Positive control for anti-hNu in human bone marrow cells. (Q) Homing of IDPSCs in muscles (injured site). Nuclei of cells counterstained with eosin. (A–H) Confocal microscopy. (I–Q) Light microscopy. Scale bars: 10 μm (A–A2, E–E2, I–Q), 20 μm (B–D, F–H).

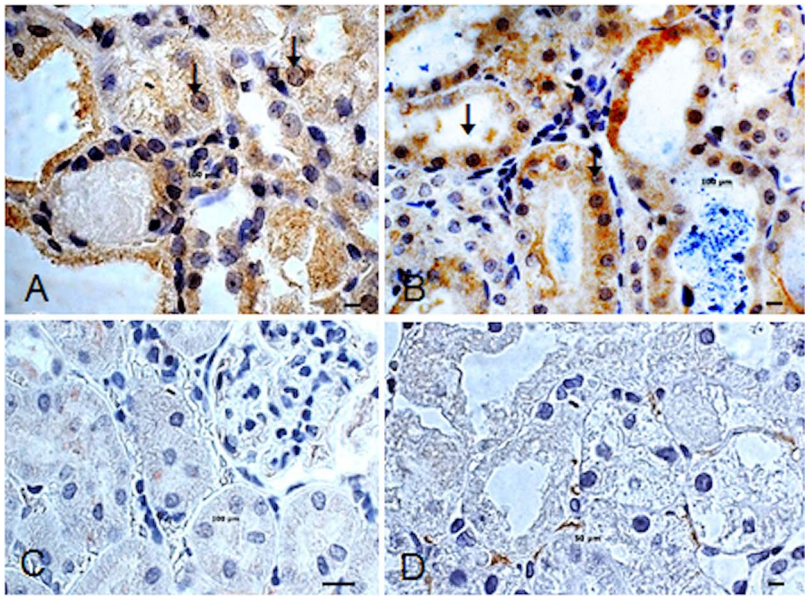

Figure 6. Effect of IDPSC transplantation on kidney cell proliferation. Ki-67 immunoreactivity observed after IP (A) and EV (B) IDPSC administration in groups B2 and B3, respectively. (C and D) Control animals from groups A and B1, respectively, are shown. Both showed either a little (D, intertubular cells) or no immunoreactivity with Ki-67 antibody. Arrows in (A) and (B) indicate Ki-67 antigen nuclear localization (brown). Light microscopy. Scale bars: 10 μm (A–D).

preferential migration to the kidney after their EV injection in ARF mice, with increased expression of hyaluronic acid (HA) (20). IDPSCs also express CD44, and this factor can play an important role in cell migration directed at injured kidneys, when compared with other studied organs such as the lungs, liver, and muscles.

Homing of stem cells occurs via their capture by the vasculature of tissues, following their transmigration across the endothelium and reaching the stromal tissue in an injured region of the target organ. After homing to the target organ, stem cells start to produce a wide range of cytokines and growth factors such as anti-inflammatory, angiogenic, antiapoptotic, and others, thus promoting their therapeutic and reparative endogenous effects (24). Almost all IDPSCs express endoglin (CD105), which is a common MSC marker (4). The cell surface glycoprotein is overexpressed on the vascular endothelium of angiogenic tissues and is upregulated by hypoxia. Hence, CD105 was suggested for use as a therapeutic target in anticancer clinical settings (11,13,14). It is plausible that the homing of IDPSCs within injured tissue, which undergoes a strong inflammatory process, is due to the expression of CD105.

Dysfunction and loss of tubular epithelial cells play central roles in the process underlying the failure of the kidney after ARF. In the present study, the effect of engrafted IDPSCs on tubular cell regeneration was explored by analyzing the proliferation marker Ki-67. In normal control kidneys and in glycerol-treated rat low numbers of Ki-67-positive cells (2–5%) were detected, indicating low frequency of tubular cell turnover. The numbers of Ki-67-positive cells in kidneys of glycerol-treated mice were significantly higher: 15% in B2 and in 28% B3 groups, compared with normal control group A: 5%. The effects of IDPSCs on cell proliferation in ARF rat model resulted in three- (B2) and fourfold (B3) increases in tubular cell proliferation.

IDPSCs were able to express VEGF after homing to injured kidneys, thus complying with the function of pericytes (8). This finding is also reinforced by the expression of both CD146 (marker for pericytes) and STRO-1 (marker for stromal cells) in IDPSCs that homed to kidney tissues after transplantation. Our study addressed important issues, which have escaped the previous attention and wide discussion of investigators. A subpopulation of human perivascular cells that show in situ pericytes and MSC immunophenotypes such as $CD146^{+}$, $CD34^{-}$, $CD45^{-}$, and $CD56^{-}$ following subsequent in vitro expansion have been isolated. These cells undergo in vitro mesodermal lineage differentiation, which are hallmarks of MSC identity (8). Hence, Caplan suggested that all MSCs are pericytes (but not all pericytes are MSCs) (5). It is interesting that IDPSCs, which anatomically are of neural crest origin, contain a subpopulation of pericytes (~36%) with appropriate phenotypes (35). In the present study, we found that all IDPSCs that homed to injured kidneys expressed CD146. This finding raises some questions: Does a pericyte subpopulation of IDPSCs show selective migration to an injured site? Alternatively, do IDPSCs migrate selectively to the kidneys due to CD44 expression and, when homed, start to express CD146 under the influence of the local environment?

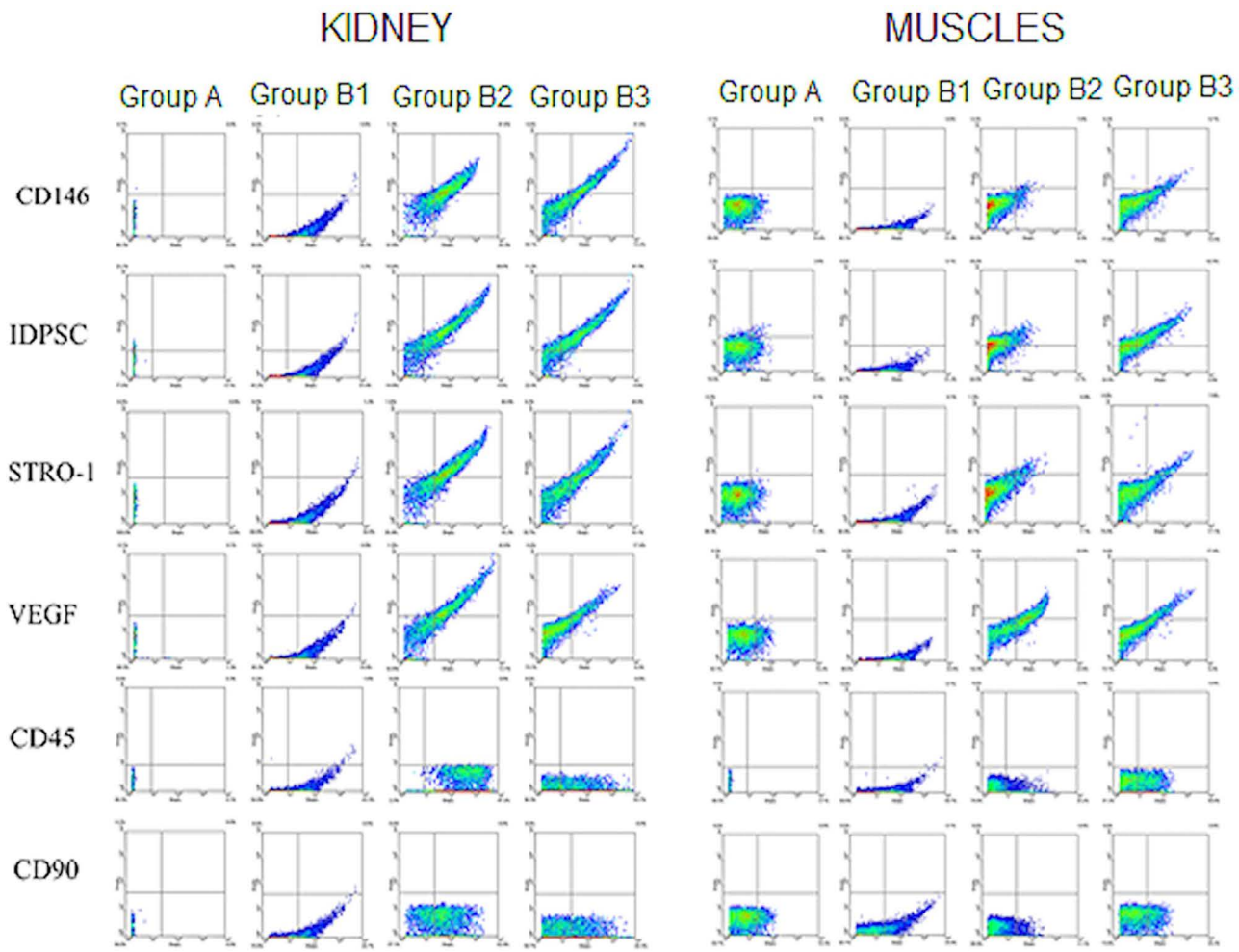

Figure 7. Flow cytometry analysis of transplanted IDPSCs in kidneys and muscle. Flow cytometry demonstrating the levels of expression of several anti-human antibodies such as CD146, IDPSC, STRO-1, VEGF, CD45, and CD90 by IDPSCs after transplantation in rat kidneys and muscle.

During vascular transit, the cells may escape and home to other organs such as the lungs, liver, and spleen, leading to a significant decrease in the number of cells able to reach the injured site (24). Previous studies revealed that the injected MSCs showed engraftment between 2.0% and 22.0% of cells, demonstrating that the direct engraftment of exogenously administered MSCs is not the only mechanism to enhance renal repair (20, 21,29). In an ARF in rat model, it has been shown that BM-MSCs home to the lungs when administrated EV, which did not occur when they were administered intra-arterially (39).

Two administration routes (IP and EV) were tested and, when compared with the other organs studied, both resulted in elevated IDPSC homing to kidney tissues. As expected, a relatively high percentage of IDPSCs were found in the liver, especially when these cells were administrated EV. Far fewer cells were detected in the muscles (glycerol injection site). However, the low percentage of IDPSCs in the lungs can probably be explained by the different properties of MSCs derived from bone marrow and dental pulp. Another issue that needs to be investigated is that, independent of the administration route, the number of cells that reached the kidneys is almost equal in all studied animals. Does this mean that the amount of cells that can be accepted by an injured organ is controlled in some way by the organ and/or by the organism? If so, does this mean that the number of cells used in particular stem cell therapies can be reduced?

Inflammation is a factor that has adverse consequences on tubule function and viability, resulting in reduction of local blood flow to the outer medulla in ARF (3). Our histological results demonstrated increased blood flow in the capillaries after IDPSC injection into the target organ, compared with the control animals. This suggests a possible anti-inflammatory role of these cells.

Immunoincompatibility is the most important concern for the clinical application of stem cells. The rejection of

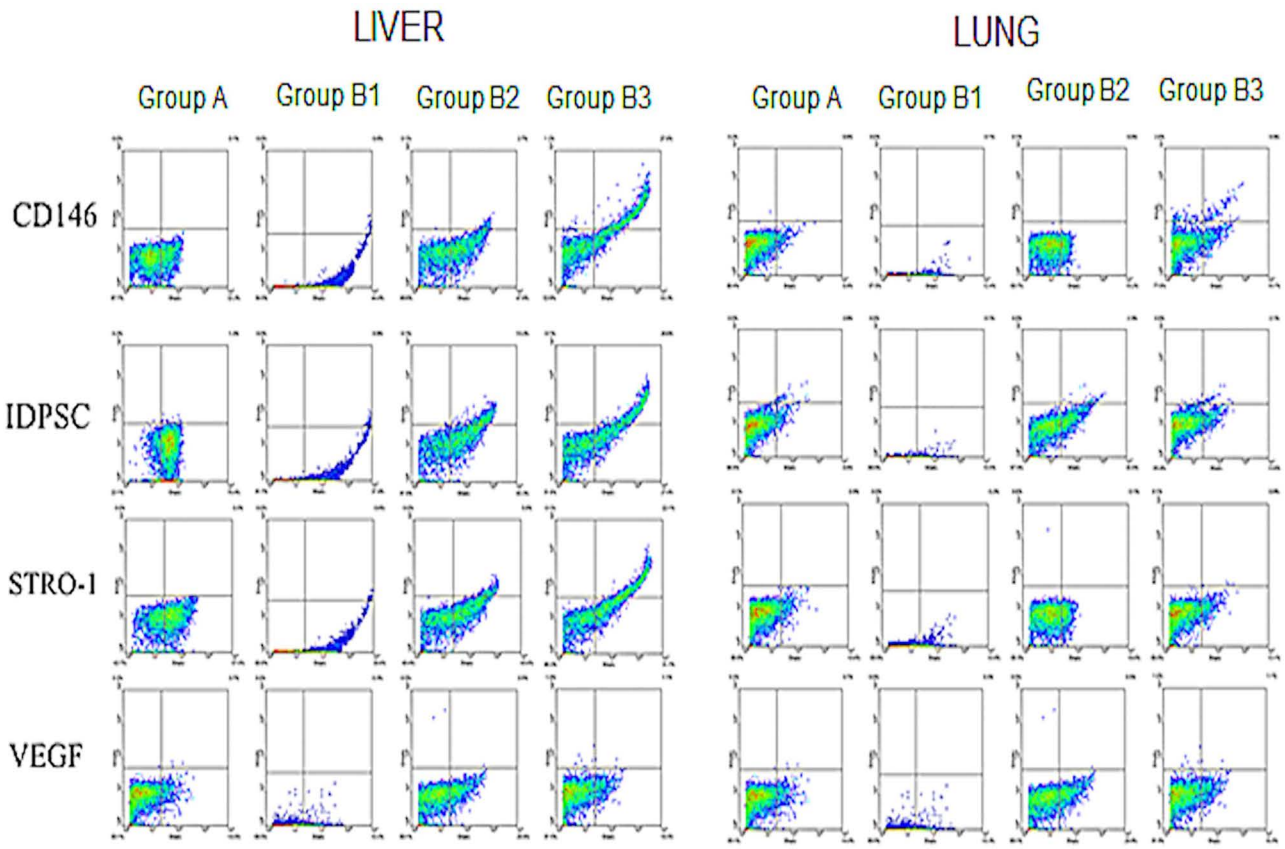

Figure 8. Flow cytometry analysis of transplanted IDPSCs in livers and lungs. Flow cytometry demonstrating the levels of expression of several anti-human antibodies such as CD146, IDPSCs, STRO-1, and VEGF by IDPSCs after transplantation in rat livers and lungs.

Table 1. Statistical Analysis of IDPSCs (%) Labeled by Different Antibodies

Application Route	Liver*	Muscle	Lung	Kidney
Antibody CD146				
Control†	$0.20^{B,a}$	$0.10^{A,a}$	$0.70^{A,a}$	$0.00^{B,a}$
Glycerol	$0.30^{B,a}$	$0.05^{A,a}$	$0.10^{A,a}$	$0.45^{B,a}$
Intraperitoneal	$2.95^{B,b}$	$0.90^{A,b}$	$0.10^{A,b}$	$31.80^{A,a}$
Endovenous	$23.20^{A,a}$	$3.40^{A,b}$	$2.95^{A,b}$	$30.90^{A,a}$
Antibody IDPSC				
Control	$3.00^{AB,a}$	$0.80^{A,a}$	$2.50^{A,a}$	$0.00^{B,a}$
Glycerol	$0.35^{B,a}$	$0.00^{A,a}$	$0.05^{A,a}$	$0.50^{B,a}$
Intraperitoneal	$9.10^{AB,b}$	$1.35^{A,b}$	$1.85^{A,b}$	$33.25^{A,a}$
Endovenous	$19.05^{A,ab}$	$6.30^{A,b}$	$2.00^{A,c}$	$34.10^{A,a}$
Antibody STRO				
Control	$1.20^{B,a}$	$0.10^{A,a}$	$0.50^{A,a}$	$0.00^{B,a}$
Glycerol	$0.20^{B,a}$	$0.05^{A,a}$	$0.05^{A,a}$	$0.65^{B,a}$
Intraperitoneal	$9.85^{AB,b}$	$3.00^{A,b}$	$0.20^{A,b}$	$37.55^{A,a}$
Endovenous	$23.90^{A,a}$	$4.85^{A,b}$	$0.90^{A,b}$	$29.40^{A,a}$
Antibody VEGF				
Control	$3.00^{A,a}$	$0.40^{A,a}$	$0.70^{A,a}$	$0.20^{B,a}$
Glycerol	$0.30^{A,a}$	$0.00^{A,a}$	$0.10^{A,a}$	$0.60^{B,a}$
Intraperitoneal	$4.55^{A,b}$	$12.00^{A,ab}$	$0.40^{A,b}$	$36.50^{A,a}$
Endovenous	$21.50^{A,ab}$	$8.15^{A,b}$	$1.85^{A,b}$	$33.80^{A,a}$

CD146, cluster of differentiation 146; IDPSC, immature dental pulp stem cell; STRO, stromal cell marker; VEGF, vascular endothelial growth factor.
*Means in the same column and followed by the same capital letter do not differ at 1% probability by Bonferroni test.
†Means in the same row and followed by the same lowercase letter do not differ at 1% probability by Bonferroni test.

donor stem cells can interfere with the normal functions of the host immune system. To avoid such rejection immunosuppressive agents are used. However, we reported in various preclinical studies that hIDPSCs showed absence of immunogenic response (9,10,16,25). In the present work, we confirmed that IDPSCs are well tolerated by the rat, allowing good survival of these cells. The evaluation of functional improvements following IDPSC transplantation was not the goal of the present study. It was also difficult due to the design of the experiment (Fig. 1) and the severity of the kidney lesion.

Overall, we demonstrated that IDPSCs are able to maintain their stem cell properties after long periods of cryopreservation and efficiently deliver a trophic effect to the site of injury in the kidneys (expression of VEGF, mitogenic, and anti-inflammatory effects) similar to pericytes and BM-MSCs (5,6). Our findings indicate that IDPSCs can contribute to the recovery of the kidney during ARF. In the context of regenerative therapies, renotropic preparations of autologous adult stem cells can be proposed as a safe strategy in humans. It seems that the stem cell phenotype plays an important role in cell delivery directed to an injured organ. Since the efforts of the investigators were directed at isolating an unlimited source of cells resembling the renal progenitors, it was shown that IDPSCs are a promising cell type for ARF. This work raised several questions that should be answered before studying the clinical benefits of any stem cells, including IDPSCs, for the treatment of ARF.

ACKNOWLEDGMENTS: We thank Drs. Enrico J. C. Santos and Ana L. Reginato from Butantan Institute, São Paulo, Brazil, for technical assistance during the development of the project, as well as Dr. Arnold Caplan from Case Western Reserve University, Cleveland, OH, USA, for the supply of antibodies and precious help. This study was supported by CAPES. The authors declare no conflicts of interest.

REFERENCES

1. Beltrão-Braga, P. I.; Pignatari, G. C.; Maiorka, P. C.; Oliveira, N. A.; Lizier, N. F.; Wenceslau, C. V.; Miglino, M. A.; Muotri, A. R.; Kerkis, I. Feeder-free derivation of induced pluripotent stem cells from human immature dental pulp stem cells Cell Transplant. 20:1707–1719; 2011.
2. Bi, B.; Schmitt, R.; Israilova, M.; Nishio, H.; Cantley, L. G. Stromal cells protect against acute tubular injury via an endocrine effect. J. Am. Soc. Nephrol. 18:2486–2496; 2007.
3. Bonventre, J. V. Mechanisms of acute kidney injury and repair. In: Jörres, A.; Ronco, C.; Kellum, J. A., eds. Management of acute kidney problems. Berlin, Germany: Springer-Verlag; 2010:13–20.
4. Caplan, A. I. Adult mesenchymal stem cells for tissue engineering versus regenerative medicine. J. Cell. Physiol. 213:341–347; 2007.
5. Caplan, A. I. All MSCs are pericytes? Cell Stem Cell 3:229–230; 2008.
6. Caplan, A. I.; Correa, D. The MSC: An injury drugstore. Cell Stem Cell 9:11–15; 2011.
7. Carraro, G.; Perin, L.; Sedrakyan, S.; Giuliani, S.; Tiozzo, C.; Lee, J.; Turcatel, G.; De Langhe, S. P.; Driscoll, B.; Bellusci, S.; Minoo, P.; Atala, A.; De Filippo, R. E.; Warburton, D. Human amniotic fluid stem cells can integrate and differentiate into epithelial lung lineages. Stem Cells 26:2902–2911; 2008.
8. Crisan, M.; Yap, S.; Casteilla, L.; Chen, C. W.; Mirko, C.; Park, T. S.; Andriolo, G.; Sun, B.; Zheng, B.; Zhang, L.; Norotte, C.; Teng, P. N.; Traas, J.; Schugar, R.; Deasy, B. M.; Badylak, S.; Buhring, H. J.; Giacobino, J. P.; Lazzari, L.; Huard, J.; Péault, B. A perivascular origin for mesenchymal stem cells in multiple human organs. Cell Stem Cell 3:301–313; 2008.
9. de Almeida, F. M; Marques, S. A.; Ramalho, B. dos S.; Rodrigues, R. F.; Cadilhe, D. V.; Furtado, D.; Kerkis, I.; Pereira, L. V.; Rehen, S. K.; Martinez, A. M. Human dental pulp cells: A new source of cell therapy in a mouse model of compressive spinal cord injury. J. Neurotrauma 28:1939–1949; 2011.
10. de Mendonça Costa, A.; Bueno, D. F.; Martins, M. T.; Kerkis, I.; Kerkis, A.; Fanganiello, R. D.; Cerruti, H.; Alonso, N.; Passos-Bueno, M. R. Reconstruction of large cranial defects in nonimmunosuppressed experimental design with human dental pulp stem cells. J. Craniofac. Surg. 19:204–210; 2008.
11. Duff, S. E.; Li, C.; Garland, J. M.; Kumar, S. CD105 is important for angiogenesis: Evidence and potential applications. FASEB J. 17:984-991; 2003.
12. Duffield, J. S.; Bonventre, J. V. Kidney tubular epithelium is restored without replacement with bone marrow-derived cells during repair after ischemic injury. Kidney Int. 68:1956–1961; 2005.
13. Fonsatti, E.; Altomonte, M.; Nicotra, M. R.; Natali, P. G.; Maio, M. Endoglin (CD105): A powerful therapeutic target on tumor-associated angiogenetic blood vessels. Distal tubular epithelial cells of the kidney: Potential support for proximal tubular cell survival after renal injury. Int. J. Biochem. Cell Biol. 39:1551–1561; 2007.
14. Fonsatti, E.; Maio, M. Highlights on endoglin (CD105): From basic findings towards clinical applications in human cancer. J. Transl. Med. 2:1479–5876; 2004.
15. Gobe, G. C.; Johnson, D. W. Distal tubular epithelial cells of the kidney: Potential support for proximal tubular cell survival after renal injury. Int. J. Biochem. Cell Biol. 39:1551–1561; 2007.
16. Gomes, J. A.; Geraldes Monteiro, B.; Melo, G. B.; Smith, R. L.; Cavenaghi Pereira da Silva, M.; Lizier, N. F.; Kerkis, A.; Cerruti, H.; Kerkis, I. Corneal reconstruction with tissue-engineered cell sheets composed of human immature dental pulp stem cells. Invest. Ophthalmol. Vis. Sci. 51:1408–1414; 2010.
17. Gupta, S.; Verfaillie, C.; Chmielewski, D.; Kren, S.; Eidman, K.; Connaire, J.; Heremans, Y.; Lund, T.; Blackstad, M.; Jiang, Y.; Luttun, A.; Rosenberg, M. E. Isolation and characterization of kidney-derived stem cells. J. Am. Soc. Nephrol. 17:3028–3040; 2006.
18. Harari-Steinberg, O.; Pleniceanu, O.; Dekel, B. Selecting the optimal cell for kidney regeneration. Fetal, adult or reprogrammed stem cells. Organogenesis 7:123–134; 2011.
19. Hauser, P. V.; De Fazio, R.; Bruno, S.; Sdei, S.; Grange, C.; Bussolati, B.; Benedetto, C.; Camussi, G. Stem cells derived from human amniotic fluid contribute to acute kidney injury recovery. Am. J. Pathol. 177:2011–2002; 2010.

20. Herrera, M. B.; Bussolati, B.; Bruno, S.; Fonsato, V.; Romanazzi, G. M.; Camussi, G. Mesenchymal stem cells contribute to the renal repair of acute tubular epithelial injury. Int. J. Mol. Med. 14:1035–1041; 2004.
21. Herrera, M. B.; Bussolati, B.; Bruno, S.; Morando, L.; Romanazzi, G. M.; Camussi, G. Exogenous mesenchymal stem cells localize to the kidney by means of CD44 following acute tubular injury. Kidney Int. 72(4):430–441; 2007.
22. Humphreys, B. D.; Valerius, M. T.; Kobayashi, A.; Mugford, J. W.; Soeung, S.; Duffield, J. S.; McMahon, A. P.; Bonventre, J. V. Intrinsic epithelial cells repair the kidney after injury. Cell Stem Cell 2:284–229; 2008.
23. Johnstone, B.; Hering, T. M.; Caplan, A. I.; Goldberg, V. M.; Jung, J. U. In vitro chondrogenesis of bone marrow-derived mesenchymal progenitor cells. Exp. Cell Res. 238:265–272; 1998.
24. Karp, J. M.; Teo, G. S. L. Mesenchymal stem cell homing: The devil is in the details. Cell Stem Cell 4:206–216; 2009.
25. Kerkis, I.; Kerkis, A.; Dozortsev, D.; Stukart-Parsons, G. C.; Gomes Massironi, S. M.; Pereira, L.V. Isolation and characterization of a population of immature dental pulp stem cells expressing OCT-4 and other embryonic stem cell markers. Cells Tissues Organs 18:4105–4116; 2006.
26. Lizier, N. F.; Kerkis, A.; Gomes, C. M.; Hebling, J.; Oliveira, C. F.; Caplan, A. I.; Kerkis, I. Scaling-up of dental pulp stem cells isolated from multiple niches. PLoS One 7:e39885; 2012.
27. Morigi, M.; Imberti, B.; Zoja, C.; Corna, D.; Tomasoni, S.; Abbate, M.; Rottoli, D.; Angioletti, S.; Benigni, A.; Perico, N.; Alison, M.; Remuzzi, G. Mesenchymal stem cells are renotropic, helping to repair the kidney and improve function in acute renal failure. J. Am. Soc. Nephrol. 15:1794–1804; 2004.
28. Patschan, D.; Patschan, S.; Muller, G. A. Endothelial progenitor cells in acute ischemic kidney injury: Strategies for increasing the cells' renoprotective competence. Int. J. Nephrol. 2011:828369; 2011.
29. Perin, L.; Sedrakyan, S.; Giuliani, S.; Da Sacco, S.; Carraro, G.; Shiri. L.; Lemley, K. V.; Rosol, M.; Wu, S.; Atala, A.; Warburton, D.; De Filippo, R. E. Protective effect of human amniotic fluid stem cells in an immunodeficient mouse model of acute tubular necrosis. PLoS One 5:e9357; 2010.
30. Pino, C. J.; Humes, H. D. Stem cell technology for the treatment of acute and chronic renal failure. Transl. Res. 156:161–168; 2010.
31. Pleniceanu, O.; Harari-Steinberg, O.; Dekel, B. Concise review: Kidney stem/progenitor cells: Differentiate, sort out, or reprogram? Stem Cells 28:1649–1659; 2010.
32. Semedo, P.; Palasio, C. G.; Oliveira, C. D.; Feitoza, C. Q.; Gonēalves, G. M.; Cenedeze, M. A.; Pacheco-Silva, A.; Câmara, N. O. Early modulation of inflammation by mesenchymal stem cell after acute kidney injury. Int. Immunopharmacol. 9:677–682; 2009.
33. Semedo, P.; Wang, P. M.; Andreucci, T. H.; Cenedeze, M. A.; Teixeira, V. P. A.; Reis, M. A.; Pacheco-Silva, A.; Câmara, N. O. S. Mesenchymal stem cells ameliorate tissue damages triggered by renal ischemia and reperfusion injury. Transplant. Proc. 39:421–423; 2007.
34. Simmons, P. J.; Torok-Storb, B. Identification of stromal cell precursors in human bone marrow by a novel monoclonal antibody, STRO-1. Blood 78:55–62; 1991.
35. Siqueira da Fonseca, S. A; Abdelmassih, S.; Lavagnolli T. M. C.; Serafim, R. C.; Clemente Santos, E. J.; Mota Mendes, C.; de Souza Pereira, V.; Ambrosio, C. E.; Miglino, M. A.; Visintin, J. A.; Abdelmassih, R.; Kerkis, A.; Kerkis, I. Human immature dental pulp stem cells' contribution to developing mouse embryos: Production of human/mouse preterm chimaeras. Cell Prolif. 42:132–140; 2009.
36. Thadhani, R.; Pascual, M.; Bonventre, J. V. Acute renal failure. N. Engl. J. Med. 334:1448–1460; 1996.
37. Togel, F.; Hu, Z.; Weiss, K.; Isaac, J.; Lange, C.; Westenfelder, C. Administered mesenchymal stem cells protect against ischemic acute renal failure through differentiation-independent mechanisms. Am. J. Physiol. Renal Physiol. 289:31–42; 2005.
38. Togel, F.; Weiss, K.; Yang, Y.; Hu, Z.; Zhang, P.; Westenfelder, C. Vasculotropic, paracrine actions of infused mesenchymal stem cells are important to the recovery from acute kidney injury. Am. J. Physiol. Renal Physiol. 292:1626–1635; 2007.
39. Zonta, S.; De Martino, M.; Bedino, G.; Piotti, T.; Rampino, M.; Gregorini, F.; Frassoni, A.; Dal Canton, P.; Dionigi, M.; Alessiani, M. Which is the most suitable and effective route of administration for mesenchymal stem cell-based immunomodulation therapy in experimental kidney transplantation: Endovenous or arterial? Transplant. Proc. 42:1336–1340; 2010.
40. Zuk, P. A.; Zhu, M.; Ashjian, P.; De Ugarte, D. A.; Huang, J. I.; Mizuno, H.; Alfonso, Z. C.; Fraser, J. K.; Benhaim, P.; Hedrick, M. H. Human adipose tissue is a source of multipotent stem cells. Mol. Biol. Cell 13:4279–4295; 2002.
41. Zurovsky, Y. Models of glycerol-induced acute renal failure in rats. J. Basic Clin. Physiol. Pharmacol. 43:213–228; 1993.